G&G

Gem News International

Contributing Editors
Emmanuel Fritsch, *CNRS, Team 6502, Institut des Matériaux Jean Rouxel (IMN), University of Nantes, France* (fritsch@cnrs imn.fr)
Kenneth Scarratt, *GIA, Bangkok* (ken.scarratt@gia.edu)

COLORED STONES AND ORGANIC MATERIALS

Aquamarine with unusually strong dichroism. Recently, a transparent grayish blue oval mixed cut (figure 1) was submitted for identification at the Gem Testing Laboratory in Jaipur. The 4.49 ct stone (12.04 × 8.88 × 7.53 mm) was relatively clean to the unaided eye. Its RI of 1.582–1.590, birefringence of 0.008 with a uniaxial negative optic sign, and hydrostatic SG of 2.71 suggested a beryl, which we later confirmed with FTIR and Raman spectroscopy. The specimen's natural origin was established by planes of dendritic platelets (usually ilmenite) oriented along the basal plane and liquid fingerprints.

The stone's most striking feature was its unusually strong dichroism, displaying deep blue and pale bluish green colors (figure 2). The deep saturated blue resembled that of a top-quality sapphire. Such strong dichroism was reminiscent of Maxixe-type (irradiated) beryls, although their dichroic colors are usually deep blue and colorless. The deep saturated blue was seen along the e-ray, the pale bluish green along the o-ray. Such a pattern of color absorption is associated with aquamarine; the opposite effect occurs in Maxixe-type beryl, which appears colorless along the e-ray and deep blue along the o-ray (R. Webster, *Gems*, 5th ed., Butterworth-Heinemann, London, 1994, pp. 124–127).

Further analysis was performed with UV-Vis-NIR spectroscopy to confirm the cause of color and differentiate between aquamarine and Maxixe-type beryl. Polarized spectra (figure 3) revealed an absorption peak at approximately 427 nm along the o- and e-rays, a typical feature in aquamarine due to the presence of ferric iron (see I. Adamo et al., "Aquamarine, Maxixe-type beryl, and hydrothermal synthetic blue beryl: Analysis and identification," Fall 2008 *G&G*,

Figure 1. This 4.49 ct grayish blue aquamarine was unusual for its strikingly intense dichroism. Photo by Gagan Choudhary.

Figure 2. The dichroic aquamarine displayed unusually intense dichroism, with a deep saturated blue along the e-ray (left) and a pale bluish green along the o-ray (right). The images were taken by fixing the polarizing filter on the camera lens and rotating the polarizer 90 degrees to separate out the two directions. Photos by Gagan Choudhary.

Editors' note: Interested contributors should send information and illustrations to Justin Hunter at justin.hunter@gia.edu or GIA, The Robert Mouawad Campus, 5345 Armada Drive, Carlsbad, CA 92008.

Gems & Gemology, Vol. 50, No. 3, pp. 244–249.

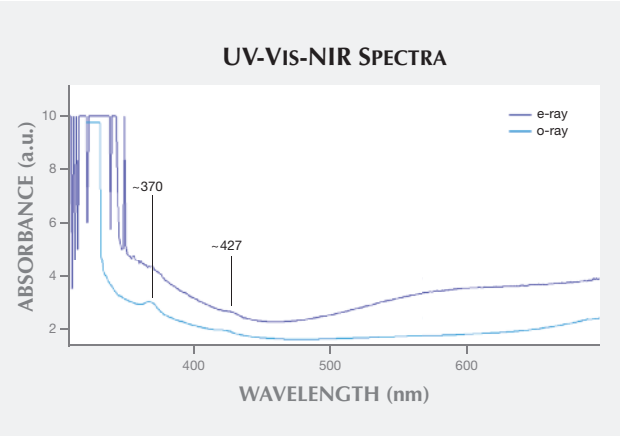

Figure 3. The aquamarine's polarized UV-Vis-NIR spectra displayed Fe^{3+}-related bands at approximately 370 and 427 nm.

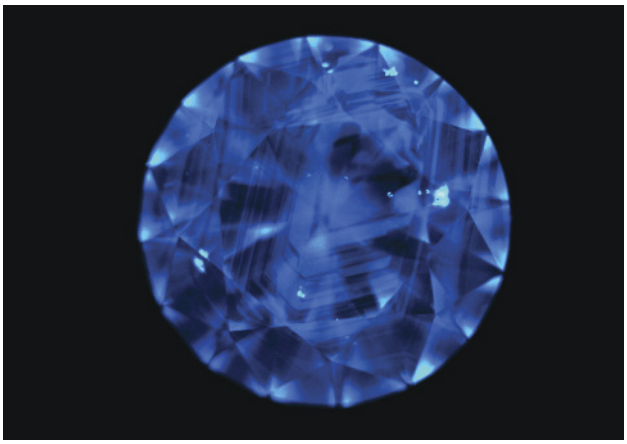

Figure 5. This DiamondView image of the host diamond shows octahedral growth zones (notice the crystal inclusions). Image by Meenakshi Chauhan.

pp. 214–226); an additional peak at about 370 nm also occurred along the o-ray. No features associated with radiation-induced color centers were present between 500 and 700 nm; these are typically observed in Maxixe-type beryls.

Standard gemological properties along with absorption spectra and the pleochroic color directions were sufficient to identify this stone as aquamarine. It displayed the most intense dichroism we have seen in an aquamarine. While there are deep sea-blue aquamarines (see O. Segura and E. Fritsch, "The Santa Maria variety of aquamarine: Never heated," *InColor*, No. 23, 2013, pp. 34–35) as well as deep blue Maxixe-type beryls, this was the deepest blue we have observed in an aquamarine with a grayish blue hue.

Gagan Choudhary (gagan@gjepcindia.com)
Gem Testing Laboratory, Jaipur, India

Color-change garnet in diamond. The Indian Gemological Institute's Gem Testing Laboratory recently examined a 0.30 ct colorless round brilliant-cut diamond containing an interesting inclusion. Infrared spectroscopy revealed features found in type IaA diamond, with a slight absorption peak due to hydrogen impurities. With a clarity grade of SI_2, the diamond contained several colorless crystals and one surface-breaking grayish green crystal (figure 4, left). Under incandescent light, the grayish green crystal appeared purplish red (figure 4, right), displaying a strong color-change phenomenon.

Under the Chelsea filter the inclusion showed a bright red reaction, suggesting the presence of chromium. There was a polished area of the included crystal on the surface, but it was too small for us to measure the refractive index.

The included crystal did not display pleochroism under microscopic observation with crossed polarizers. Viewed in immersion, it appeared to be singly refractive. DiamondView imaging showed the fluorescence pattern of growth planes found in natural diamond (figure 5). Typical octahedral growth zones of blue N3 fluorescence were evident, with no disturbance in the zones around the color-change crystal.

For conclusive identification of the inclusion, we sent the diamond to the Gem Testing Laboratory in Jaipur for laser Raman spectroscopy. As the color-change crystal

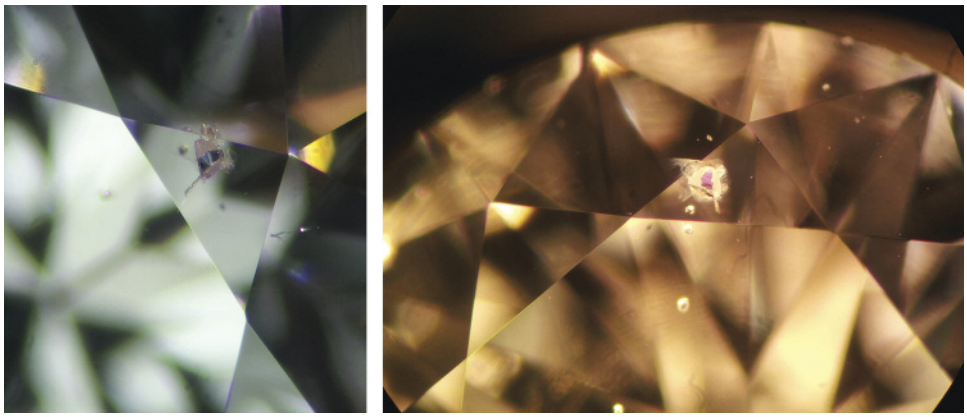

Figure 4. This inclusion, a color-change pyrope-spessartine garnet crystal in diamond, appeared grayish green in fluorescent light (left) and purplish red in incandescent light (right). Photomicrographs by Meenakshi Chauhan; field of view 2 mm (left) and 3 mm (right).

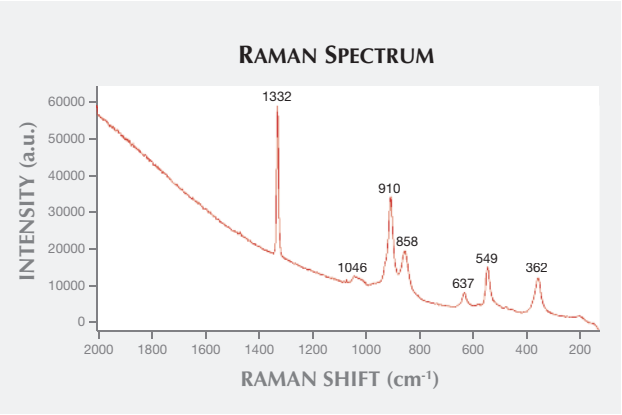

Figure 6. The Raman spectrum of the color-change pyrope-spessartine garnet inclusion showed the 1046, 910, 858, 637, 549, and 362 cm^{-1} peaks assigned to garnet. The 1332 cm^{-1} peak is assigned to diamond.

broke through the diamond's surface, a clear Raman spectrum could be obtained (figure 6). The peak at approximately 1332 cm^{-1} is assigned to diamond, and the peaks at approximately 1046, 910, 858, 637, 549, and 362 cm^{-1} are assigned to garnet. The 910 cm^{-1} peak is associated with the pyralspite isomorphous series, which is comprised of pyrope, almandine, and spessartine garnet. The inclusion was therefore identified as garnet belonging to the pyralspite series.

Meenakshi Chauhan
Indian Gemological Institute
Gem Testing Laboratory, GJEPC, New Delhi

First discovery of topazolite in Mexico. Garnet occurs in a wide variety of colors according to composition: pyrope and almandine (typically red), spessartite (brownish to orange), grossular (brown, yellow, and green), andradite (brown to black), and uvarovite (bright green). The three varieties of andradite are melanite, topazolite, and demantoid. *Topazolite*, a name that has been criticized as too similar to that of the gem species topaz, is a greenish yellow to yellow-brown andradite. According to some studies (e.g., C.M. Stockton and D.V. Manson "Gem andradite garnets," Winter 1983 *G&G*, pp. 202–208), it rarely occurs in crystals large enough to be faceted.

In January 2014, during mineralogical investigations of Mexican garnet, we made the first reported discovery of fine topazolite crystals in Mexico. These yellow to yellow-brown crystals, measuring 1.5–2.5 cm, are hosted by the Las Vigas skarn deposits (the Cerro de la Concordia mine in Las Vigas de Ramirez municipality and the Piedra Parada mine in Tatatila municipality). The deposits are located in Veracruz State, about 50 km southeast of the town of Valle de Veracruz.

The garnet composition was determined by electron microprobe, using a 41-point analysis and standard conditions of 20 kV, 20 mA, and 1 µm beam size on a JEOL JSM-35c microprobe. We chose a euhedral, relatively homogeneous crystal about 1 cm in diameter from the specimen shown in figure 7. Measurement time was 30 seconds on the peak center. The standards used were MgO for Mg, Al_2O_3 for Al, jadeite for Si, wollastonite for Ca, and elemental Fe and Mn. The electron microprobe analyses showed little compositional variation or zoning. We calculated the structural formula on the basis of 12 oxygen atoms, with the assumption of all iron as ferric. The approximate composition averaged $(Ca_{2.86}Mg_{0.06}Mn_{0.02})_{2.94}(Al_{1.20}Fe^{3+}_{0.72})_{1.92}Si_{3.03}Ti_{0.05}O_{12}$, which may be expressed as $Gr_{60.50}And_{36.70}Py_{2.80}$.

UV-visible spectroscopy showed absorption bands at 375, 416, 442, 497, and 584 nm, which can be assigned to the spin-forbidden crystal-field transition of Fe^{3+} substituted on the octahedral Al^{3+} site of the garnet structure. The correlated set of these bands also show a pattern close to that characteristic of a d^5 trivalent ion in octahedral oxygen coordination. The Mössbauer spectra were characterized by a sharp, slightly asymmetric ferrous doublet. The UV-visible and Mössbauer spectra are comparable to those reported for some garnets in previous reports (A.S. Marfunin, Ed., *Advanced Mineralogy*, Vol. 2, Springer-Verlag, Berlin, 1995, pp. 74–75, 114).

The three samples of rough topazolite (measuring 1.0–1.5 cm in longest dimension) gave the following properties: yellow-brown color; isotropic and weakly anisotropic; weak strain birefringence; RI—n_α = 1.84–1.89; hydrostatic SG—3.75–3.85; and fluorescence—inert to both long- and short-wave UV radiation.

This Mexican topazolite deposit has not been mined, and in the absence of detailed geological, mineralogical, and gemological study, no estimate of the reserves is avail-

Figure 7. This topazolite specimen is from a recent discovery in the Mexican state of Veracruz. Photo by Cristobal Castillo.

Figure 8. This giant clam pearl was recovered from a Tridacna gigas *mollusk in Papua New Guinea. Photo by Lai Tai-An Gem Lab.*

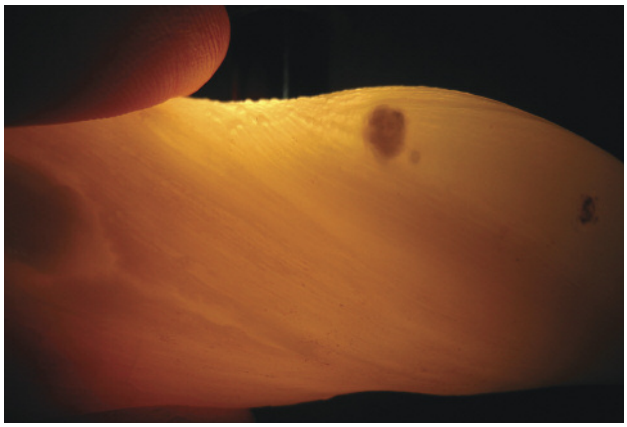

Figure 10. The Tridacna *pearl exhibited pronounced banding when viewed with transmitted light. Photo by Lai Tai-An Gem Lab.*

able. For now, there are no specimens or fashioned material from Las Vigas in the Mexican lapidary market.

Mikhail Ostrooumov (ostroum@umich.mx)
Institute of Earth Sciences (INICIT)
University of Michoacan, Morelia, Mexico

A large baroque *Tridacna gigas* (giant clam) pearl. Natural pearls from various clam species are not as rare as many believe, and plenty of samples are available in the market. But with the exception of a few very large specimens, they tend to occur in sizes under 20 carats. A client of the Lai Tai-An Gem Lab in Taipei recently requested a report on what he claimed was a natural clam pearl (figure 8) recovered from a huge *Tridacna gigas* mollusk from a fishery in Papua New Guinea in 1981.

The pearl exhibited an elongated baroque shape with uneven brown and white coloration, lacking the lustrous and shimmering iridescent colors of a nacreous pearl. It weighed 360.59 ct and measured 76.7 × 28.0 × 25.8 mm. We also recorded an SG of 2.88, which fell within the range of other *Tridacna* pearls examined in our laboratory. Long-wave UV produced a moderate chalky blue reaction. FTIR, Raman, and UV-visible spectra were collected. The Raman spectrum clearly showed that the pearl was composed of aragonite, given the peaks at approximately 142, 199, 701, and 1082 cm^{-1}. FTIR reflectance spectra also revealed calcium carbonate in the form of aragonite, with peaks at approximately 873 and 1483 cm^{-1}.

Figure 9. The natural Tridacna *pearl showed a characteristic sugary surface texture. Photo by Lai Tai-An Gem Lab; magnified 60×.*

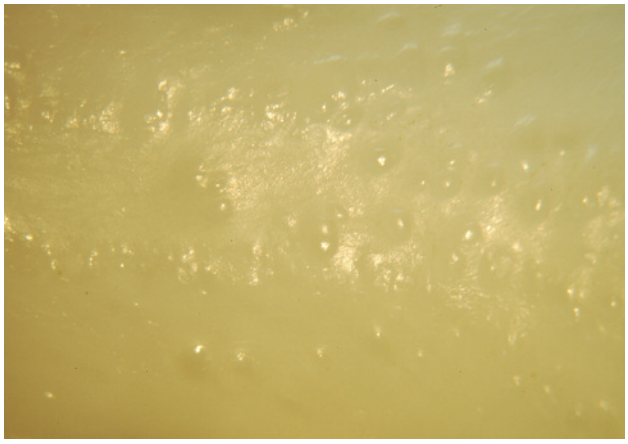

While microradiography is usually applied to the identification of pearls, it is considered especially beneficial when various types of nacreous pearls need to be separated from one another. It is usually less helpful with non-nacreous or non-porcelaneous pearls such as this one, since many reveal little in the way of helpful structure. Observed through the loupe and microscope, the pearl showed the grainy or sugary surface texture (figure 9) typical of some natural *Tridacna* pearls. This example was noteworthy for its size and interesting coloration, and its pronounced banding when viewed with transmitted light (figure 10), a feature that is often considered indicative of shell fashioned into imitation pearls. This *Tridacna* pearl was clearly no imitation.

Larry Tai-An Lai (service@laitaian.com.tw)
Lai Tai-An Gem Laboratory, Taipei

TREATMENTS

Coated fire opal in the Chinese market. Fire opal is an attractive variety of gem opal characterized by its red-orange-yellow bodycolor, with or without play-of-color. Since about 2013, the Chinese market has seen an increase in natural, synthetic (sold as Mexifire), and treated fire opals, posing identification challenges for the gemologist.

At the July 2014 Beijing Jewelry Fair, a fire opal with a rather unusual orange bodycolor (figure 11) attracted our

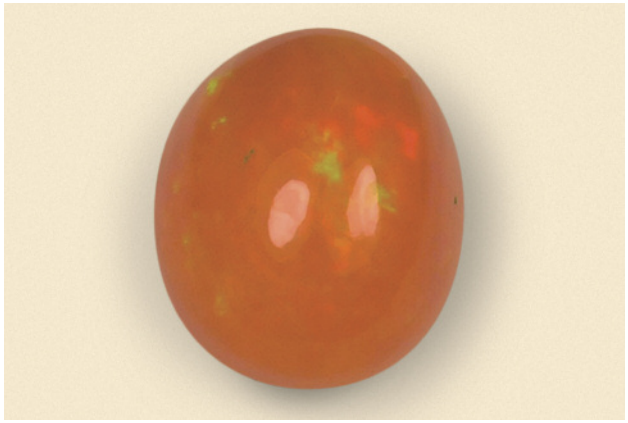

Figure 11. This 3.87 ct translucent orange fire opal with play-of-color was identified as a coated stone. Photo by Wen Han.

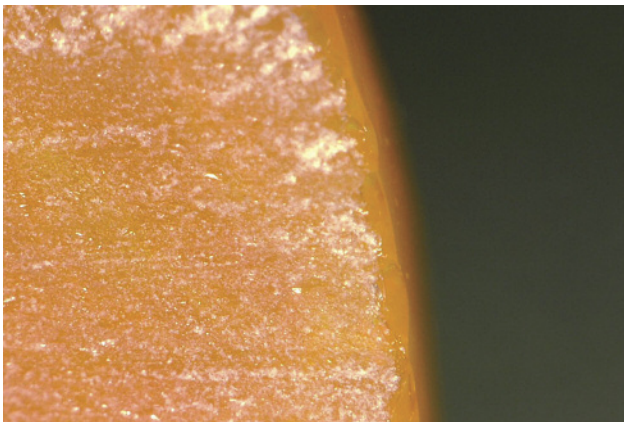

Figure 13. A cross-section image of the fire opal shows a coated surface layer about 60–90 µm thick. Photo by Wen Han; magnified 100×.

interest. It was a 3.87 ct oval cabochon with fair play-of-color, measuring approximately 14 × 10 × 6 mm. Its spot RI of about 1.39 and hydrostatic SG of 1.85 were both lower than the values for most natural fire opal. It was inert to both long- and short-wave UV radiation; untreated fire opal may also be inert to UV radiation or show green and blue fluorescence. Magnification revealed obvious scratching and small pits on the surface (figure 12), suggesting a lower hardness and the presence of a coating. We cut the sample in half for further examination. High magnification clearly showed the boundary between the orange layer and the substrate, which was also orange opal. The coated layer was about 60–90 µm thick (figure 13).

EDXRF chemical analysis detected mainly Si and minor amounts of Ca, Na, and K. Fourier-transform infrared (FTIR) and Raman spectroscopy were used to identify the coating. Infrared reflectance spectroscopy revealed three strong bands at 1099, 789, and 474 cm^{-1} that are related to the fundamental Si-O vibrations, as expected for natural fire opal. Then we scraped off the coating with a razor blade to obtain its infrared transmittance spectrum. The peaks, specifically those at 2926, 1729, 1451, and 1159 cm^{-1}, indicated the presence of organic matter consistent with acrylic polymer (figure 14). The Raman scattering spectra of the fire opal revealed several peaks attributed to both the substrate opal and the coating (figure 15). The Raman bands at about 350, 785, and 1080 cm^{-1}, due to different stretching and bending vibration modes of the Si-O system, are typical for opal-CT. Other peaks, including 1320 and 1610 cm^{-1}, are attributed to the acrylic coating material. Acrylic coatings are applied to various gem materials, such as lapis lazuli and jadeite (Summer 1992 Gem News, p. 135). This coating of acrylic polymer was used to enhance the fire opal's color and seal its fissures. The coating also lowered the stone's RI and SG values.

Our investigation, believed to be the first report of coated fire opal in the Chinese market, reinforces the need

Figure 12. Surface scratches and small pits were visible on the coated fire opal. Photo by Wen Han.

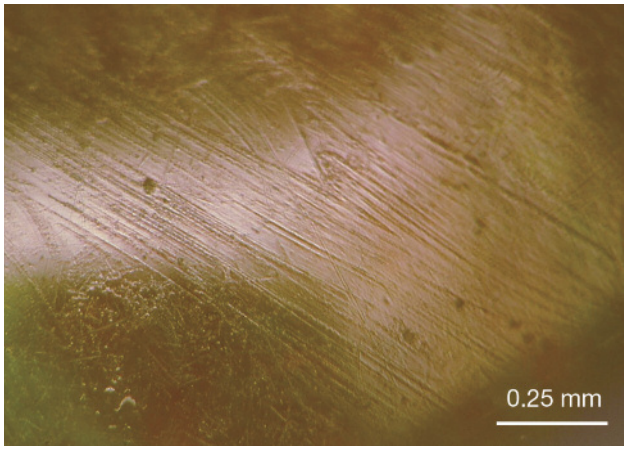

Figure 14. The FTIR spectrum of the coating scraped from the surface of the fire opal exhibits characteristic peaks at 2926, 1729, 1451, and 1159 cm^{-1} consistent with acrylic polymer.

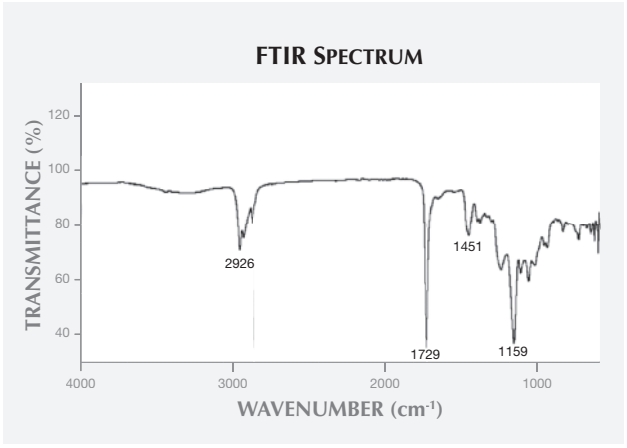

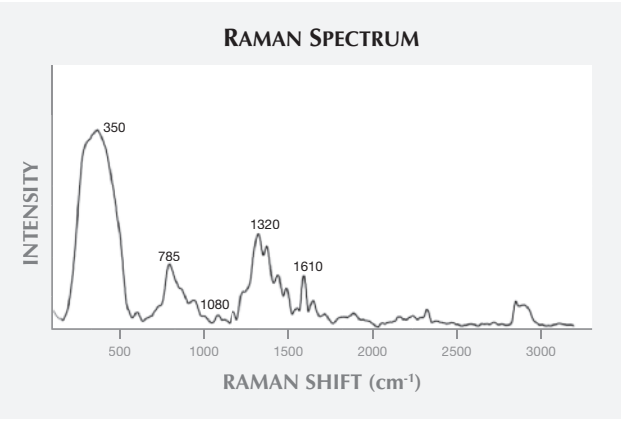

Figure 15. Raman bands at approximately 350, 785, and 1080 cm^{-1} are typical for opal-CT; the other peaks, including those at 1320 and 1610 cm^{-1}, are attributed to the acrylic coating.

for caution when buying these products. This coated fire opal's lower RI and SG values, combined with magnification and Raman spectroscopy, are effective and nondestructive means of identification.

Wen Han (winnerzx@126.com), Taijin Lu, Hua Chen, and Jian Zhang
National Gems & Jewelry Technology Administrative Center (NGTC) BeijingT

CONFERENCE REPORTS

IMA General Meeting. The 21st General Meeting of the International Mineralogical Association (IMA) was held September 1–5 in Johannesburg, South Africa. Several oral and poster presentations were presented in a session on gem materials.

Giovanna Agnosi (University of Bari, Italy) discussed preliminary results of an X-ray diffraction topography study of Colombian trapiche emeralds, which revealed a consistent crystallinity between the arms and the hexagonal core. She presented a model of trapiche formation in which the growth of the hexagonal core occurred first, followed by the six arm sections. **Ulrika D'Haenens-Johansson** (GIA, New York) outlined the status of synthetic diamond production. She reviewed the means of identification based on visual observations, structure-related ultraviolet fluorescence reactions, and distinctive spectroscopic features. In concluding, she noted that synthetic diamonds can be unequivocally recognized by major gem laboratories.

Andrew Fagan (University of British Columbia, Vancouver) presented the geologic setting and a model of formation of the Fiskenæsset corundum district in southwest Greenland. Estimates of ore reserves suggest that this could become a commercial ruby deposit. **Gaston Giuliani** (Centre de Recherches Pétrographiques et Géochimiques, Nancy, France) studied the oxygen isotope and trace-element chemistry of sapphire xenocrysts in basalts from Changle, China, and of corundum from the Mbuyi-Mayi kimberlite in the Democratic Republic of Congo, to trace their primary sources. In both cases, the host basalt and kimberlite transported the corundum crystals from the lower crust and upper mantle.

Daniel Ichang'i (University of Nairobi) described efforts by the Kenyan government to document and better understand the geologic setting of the country's numerous gem deposits. He discussed two main occurrence lithologies: the metamorphic rocks of the Neoproterozoic Mozambique orogenic belt, and the Paleogene-Neogene basaltic volcanics in the Northern and Central Kenya rift regions.

Stefanos Karampelas (Gübelin Gem Lab, Lucerne, Switzerland) detailed the gemological characteristics of emeralds from Itatitia in Minas Gerais, Brazil. The emeralds formed along the contact between phlogopite schists and highly evolved granitic pegmatites. Based on minor and trace-element chemistry, they can be distinguished from emeralds from other Brazilian and world deposits. **Vincent Pardieu** (GIA, Bangkok) gave a talk about Montepuez in northern Mozambique, which is currently the world's largest source of rubies. He also presented a short film about GIA expeditions he has led to gem deposits in eastern Africa. **Wuyi Wang** (GIA, New York) presented a study of carbon isotopes of synthetic and natural diamonds. The latter displayed $\delta^{13}C$ values from 0 to –20‰, while the former ranged from –25 to –75‰.

Christopher M. Breeding (GIA, Carlsbad, California) described the interesting features of alluvial diamonds from the Marange deposit in eastern Zimbabwe. These type Ia diamonds display surface radiation staining, aggregated nitrogen impurities, and elevated hydrogen impurity contents, but these features do not provide a reliable indicator of geographic origin. **Julien Feneyrol** (Centre de Recherches Pétrographiques et Géochimiques, Nancy, France) presented a model of the metamorphic formation of tsavorite nodules in primary deposits. The tsavorite nodules are always contained within graphitic gneiss and calc-silicates with intercalations of marble. **Elena Sorokina** (Fersman Mineralogical Museum, Moscow) described a model of ruby and sapphire formation in marbles at Snezhnoe in Tajikistan.

James E. Shigley
GIA, Carlsbad, California

ERRATA

1. The S. Saeseaw et al. emerald inclusions article in the Summer 2014 issue (pp. 114–132) listed the photomicrograph image widths ten times larger than their actual width.

2. The Summer 2014 Gem News International section (pp. 158–159) erroneously cited "absorption peaks" in the Raman spectrum of a jadeite bangle. We thank Thierry Cathelineau for bringing this to our attention.